On-board determination of the friction coefficient between tire and road using standard-application vehicle dynamics sensors

C. Lex, A. Eichberger, W. Hirschberg
Institute of Automotive Engineering, Graz University of Technology, Austria

ABSTRACT: With increasing automation of driving tasks, reliable information on the road conditions is required to ensure safe automated transport. A method is presented to determine the maximum coefficient of friction between tire and road surface during driving based on measurements of the vehicle's dynamic state using a model-based approach. Particle filtering is applied as a state estimation technique which is able to consider measurement noise and model uncertainties within a Bayesian framework. Almost only standard sensors as installed in a vehicle with electronic stability control (ESC) are used. The sensor information required includes wheel speeds, longitudinal and lateral chassis acceleration, the yaw rate, the steering wheel angle and the longitudinal velocity. Using real vehicle measurements, possibilities and limitations of the presented approach are discussed. It is demonstrated that the tire and road conditions can be estimated in many driving conditions with a high confidence.

Keywords: tire-road friction estimation, road condition, tire condition, on-board detection, vehicle dynamics, particle filtering, Bayes theorem

1 INTRODUCTION

The functionality of today's vehicles is limited, because the maximum tire-road friction coefficient during driving, which limits the maximum transmittable tire-road forces, is not known. This is especially relevant since automation of driving tasks is increasing. In case of fully automated driving, the vehicle requires knowledge on the road (and tire) conditions in order to safely transport passengers and payload through traffic in different road and weather conditions. Information on the road condition is also required for semi-automated driving functions to adapt intervention strategies or to instruct the driver to take over in a critical situation. This could be the case in presence of poor road conditions that are outside the operability of an automated control, or if a current estimate of the road conditions has too low confidence to be relied on during automated driving, e.g. (Eichberger 2011).

The maximum tire-road friction coefficient $\mu^{\max}$ is defined as the ratio between the maximum transmittable longitudinal tire force $F_x^{\max}$ und the vertical tire load F_z. It depends on tire, road and vehicle parameters, as well as on the presence and consistency of precipitation like rain or snow. During typical driving, $\mu^{\max}$ may change between 0.1 and 1 because of changes in road and weather conditions, e.g. (Gustafsson 1997).

1.1 *State of the art*

Due the importance of $\mu^{\max}$ for driving safety, its estimation has been extensively investigated. Vehicles equipped with electronic stability control (ESC) already provide a good basis of sensor signals to evaluate the vehicle's dynamic state, thus many methods focus on determining $\mu^{\max}$ based on these measurements. Among the published approaches based on vehicle dynamics, some aim to estimate $\mu^{\max}$ by comparing the measured vehicle's state to an expected one using a model-based approach. To also consider measurement noise and model uncertainties, methods within the Bayesian framework such as Kalman filtering, Bayesian state estimation and particle filtering have proven to be suitable. For example, *Gustafsson* used Kalman filtering to estimate an effect of $\mu^{\max}$ on the longitudinal tire force at small values of longitudinal slip using only measurements of the wheel speeds, (Gustafsson 1997). *Boßdorf-Zimmer* estimated both the vehicle's side-slip angle and $\mu^{\max}$ during lateral manoeuvres using extended Kalman filtering, (Boßdorf-Zimmer 2007). An adapted form of a particle filter has been used by *Ray*, who compared estimated horizontal tire forces to those expected at certain values of $\mu^{\max}$ and thus determined the most probable $\mu^{\max}$ for the current driving situation, (Ray 1997).

The present method focuses on the longitudinal dynamics of the vehicle, and especially the wheels. Like within the approach proposed by *Ray*, a particle filter has been used to determine $\mu^{\max}$ based on longitudinal tire characteristics, (Ray 1997). Other than the mentioned approach, the presented implementation enables a good compromise between an accurate estimate that may converge with time and the fast detection of changes of $\mu^{\max}$ by applying re-sampling and re-initialisation strategies.

2 METHOD

The determination of $\mu^{\max}$ based on measurements of the vehicle's states can be treated as a state estimation problem, where the vehicle's state equations are influenced by time-varying model parameter $\mu^{\max}$ which is to be observed. Therefore, a model given in the form of

$$\mathbf{x}(k) = \mathbf{f}(\mathbf{x}(k-1), \mathbf{w}(k)) \quad (1)$$

$$\mathbf{z}(k) = \mathbf{h}(\mathbf{x}(k), \mathbf{v}(k)), \quad (2)$$

with a non-linear difference equation for the state vector $\mathbf{x}(k)$ to be observed and a non-linear measurement equation $\mathbf{z}(k)$ at discrete time step k, (Simon 2006). Within this model, uncertainties due to process noise $\mathbf{w}(k)$ and measurement noise $\mathbf{v}(k)$ are also considered using prior knowledge on their statistical probability distribution, e.g. their probability density functions (PDF). The state $\mathbf{x}(k)$ includes the wheel-individual maximum coefficients of friction $\left[\mu_{fl}^{\max} \quad \mu_{fr}^{\max} \quad \mu_{rl}^{\max} \quad \mu_{rr}^{\max}\right]^{\mathrm{T}}$, with the first subscripts f, r for the front or rear wheels and l, r at the second position for left or right wheel. The measurement vector $\mathbf{z}(k)$ comprises the longitudinal tire forces $\left[F_{x,fl} \quad F_{x,fr} \quad F_{x,rl} \quad F_{x,rr}\right]^{\mathrm{T}}$ at each wheel. Rather than using a direct measurement of $\mathbf{z}(k)$, it is estimated separately based on the vehicle's dynamic reaction as shown below. Within this section, first a brief presentation of particle filtering is given. Then, the wheel and tire model used within the particle filter are described.

2.1 *Particle filtering*

Particle filters are Bayesian state estimators suitable to observe certain states of models given in the form of Equations 1 and 2, (Simon 2006). These estimators are able to deal with $\mathbf{w}$ and $\mathbf{v}$ using prior information on their statistical characteristics. Unlike Kalman filters, particle filters can also be applied to non-linear models without additional adaptation like e.g. linearisation of the non-linear equations at working point.

For each of the state variables in $\mathbf{x}$, different realistic hypotheses for its initial values are assumed. These N hypotheses of $\mathbf{x}$ are randomly generated for time step $k = 1$ using the a priori PDF of $\mathbf{x}$. The computational effort of the particle filter strongly depends on the number N of particles that is chosen. With these hypotheses $\mathbf{x}_h(k)$, model-based values $\mathbf{h}(\mathbf{x}_h(k))$ are calculated using Equation 2. Then, the relative likelihood of each of the particles is calculated. This is done by comparing the assumptions $\mathbf{h}(\mathbf{x}_h(k))$ and the measurement $\mathbf{z}(k)$ assuming a certain statistical distribution between the two, in the given case a multivariate Gaussian distribution.

The relative likelihood of unlikely states is very small and does not contribute to an estimate, but still requires computational effort for calculation of these particle's likelihoods. To counteract, a re-sampling strategy is applied. Using the relative likelihood of the prior particles, which describes the probability distribution of the particles, a new set of again N particles $\mathbf{x}^{+}(k)$ is generated.

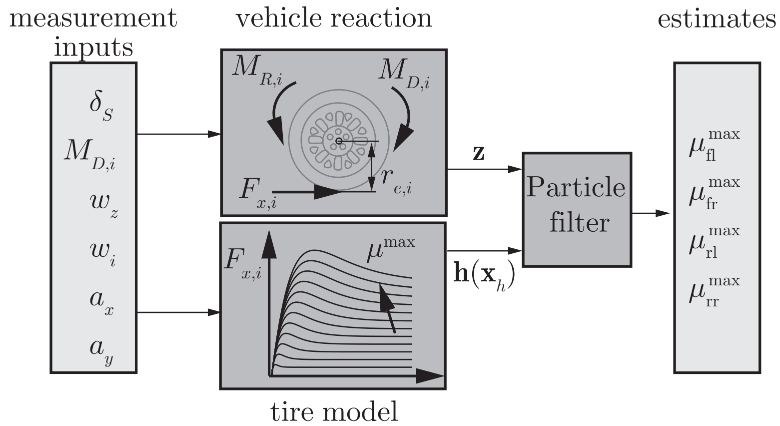

Figure 1. Schematic structure of observer including the measurement inputs, vector $\mathbf{z}$ of current longitudinal tire forces calculated based on the vehicle's reaction, vector $\mathbf{h}$ for the different particles $\mathbf{x}_h$ calculated based on a tire model and the resulting estimates $\hat{\mathbf{x}}$. Graphic depiction based on (Lex 2015).

Different strategies for re-sampling may be applied, influencing the computational effort and the convergence speed of an estimate. Finally, the most probable state is calculated by

$$\hat{\mathbf{x}}(k) = \frac{1}{N} \sum_{h=1}^{N} \mathbf{x}^{+}(k). \tag{3}$$

2.2 *Wheel and tire model*

Figure 1 shows the schematic structure of the observer used. As mentioned, the vector $\mathbf{z}$ comprises the current longitudinal tire forces $F_{x,i}$ for each of the i wheels. Using the wheels' rotational equilibrium, they are given by

$$F_{x,i}(k) = \frac{1}{r_{s,i}} \cdot \left(M_{D,i}(k) - M_{R,i} - I_i \cdot \frac{\omega_i(k) - \omega_i(k-1)}{t(k) - t(k-1)} \right). \tag{4}$$

Required inputs are the wheel's driving and braking torque $M_{D,i}$, the rolling resistance $M_{R,i}$, the wheel speeds ω_i, the wheel's moment of inertia I_i and the static tire radii $r_{s,i}$. The wheel speeds were directly measured using ESC sensors. The wheel's parameters I_i and $r_{s,i}$ were assumed constant, and $M_{R,i}$ was modelled as a function of the tire vertical load. Wheel load transfer during braking, accelerating and cornering was considered using the measured horizontal body accelerations a_x and a_y. The wheel's torque $M_{D,i}$ was being calculated with a_x using the vehicle's longitudinal equilibrium of motion, (Lex 2015).

Simultaneously to the calculation of $\mathbf{z}$, the longitudinal tire forces expected for different hypotheses or particles $\mathbf{x}_h$ of $\mu^{\max}$ are calculated for the current driving state. The vector $\mathbf{h}$ containing these expected longitudinal forces is calculated using the tire model *TMsimple*, (Hirschberg 2009). Apart from $\mu^{\max}$, the required inputs for the tire model are the wheel's longitudinal and lateral slip, as well as the vertical tire load. To calculate the wheels' longitudinal slips, the vehicle's longitudinal velocity is required. ESC sensors were not sufficient to calculate this velocity sufficiently accurate, thus in addition GPS velocity and inertial measurements had to be used. These are the only sensor signals required apart from ESC sensors.

Within this article, only results for pure longitudinal manoeuvres with the lateral slip being zero are presented. However, although not shown, combined longitudinal and lateral driving conditions are included within the estimator. Therefore, the steering wheel angle δ_S and the vehicle's yaw rate ω_z as shown in Figure 1 are also considered. Finally, $\mathbf{z}$ and $\mathbf{h}(\mathbf{x})_h$ are being compared within the particle filter in order to get the most probable value of $\hat{\mathbf{x}}$.

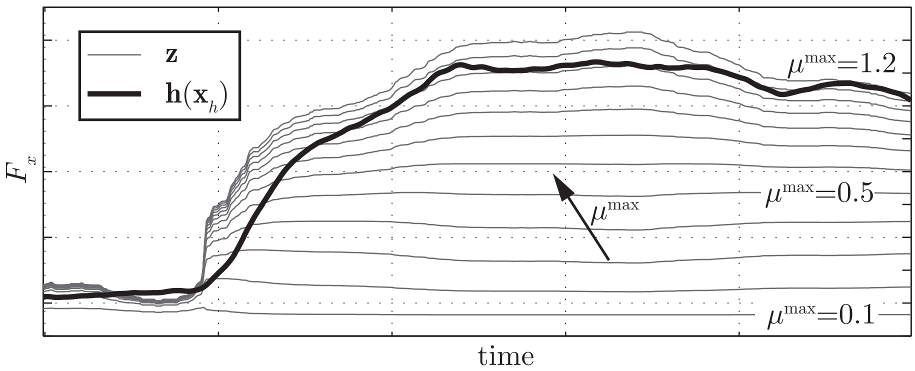

Figure 2. Representation of longitudinal tire forces over time for an exemplary driving manoeuvre, i.e. during accelerating (cf. Figure 3). The thick black line shows $\mathbf{z}$ estimated based on the wheels' dynamics, the thin grey lines show the tire model-based $\mathbf{h}$ for different $\mathbf{x}_h$, (Lex 2015).

3 RESULTS

The identification of the friction potential has been investigated using measurements from accelerating and braking manoeuvres with different dynamic excitations (e.g. maximum body accelerations) on high- and low-friction surfaces, for changing road conditions (μ *step*), and for different road conditions on left and right wheels (μ *split*). Existing methods identify the most probable estimate at every time step, e.g. (Ray 1997), without letting the estimate converge with time. This enables fast detection of changes in road and tire conditions, but is also sensitive to small deviations due to uncertainties and results in noisy estimates. To find a balance, convergence of particles was allowed in dependence of statistical characteristics of the estimate, (Lex 2015). The following results comprise both results for estimation without convergence (fixed particles), and converging particles including a re-initialisation strategy (sampled particles) enabling detection of changes. In both cases, the particles for $\mu^{\max}$ start with uniform distribution between 0.1 and 1.2.

For an exemplary driving condition, Figure 2 shows both $\mathbf{z}$ and $\mathbf{h}$ for different $\mathbf{x}_h$ over time. As described in Section 2, $\hat{\mu}^{\max}$ is estimated within the particle filter based on the estimate $\mathbf{z}$ of the longitudinal force depending on the wheels' dynamics (thick black line), and based on the model-based calculated longitudinal forces $\mathbf{h}(\mathbf{x})_h$ for different hypotheses of $\mu^{\max}$ (thin grey lines). It can be seen that there are deviations between $\mathbf{z}$ and $\mathbf{h}(\mathbf{x})_h$ at certain times, e.g. due to model and measurement uncertainties. Also, time delay due to a delayed vehicle response to an input influences the estimate can be a reason, which occurs in Figure 2 when F_x starts to increase.

3.1 *Accelerating on constant μ^{max}*

Figure 3 shows the estimation results for the front left wheel during an acceleration manoeuvre on a high-friction surface. Whereas the estimate based on fixed particles (non-converging) shows high deviations in the beginning and a noisy characteristic, the estimate using sampled particles rapidly converges. For this particular case shown in Figure 3, particles have not been re-initialised. It can be seen that the estimate does not change with time once it converged, and thus a change in friction after convergence would not be detected.

3.2 *Braking on μ step*

Figure 4 shows the estimation results for two braking manoeuvres on μ *step* conditions, both transitioning from a high- to a low-friction surface. It can be seen that with higher decelerations as shown on the left side, both estimation strategies show good results when detecting the high- and the low-friction condition as well as the transition. During gentle braking, however, the high-friction surface cannot be detected. Within the estimator, the low acceleration is being interpreted as a low-friction surface. This is undesirable for further applications, which also require information on the trustworthiness of the current estimate. Further investigations implicate that statistical characteristics of the estimate and the particles may be a useful measure for the trustworthiness of the current estimate, (Lex 2015).

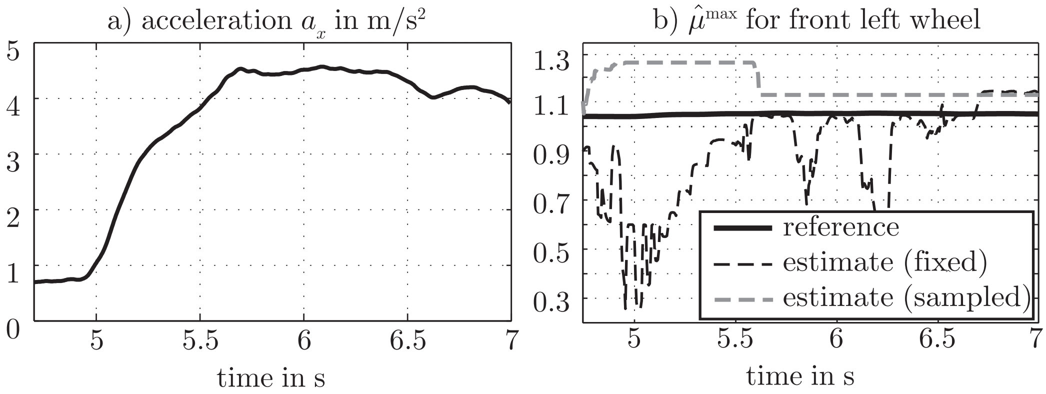

Figure 3. Estimates of $\mu^{\max}$ for front left wheel for two estimation strategies shown on right side, which were obtained during the manoeuvre shown on the right side with high positive accelerations starting at $v_x \approx 20$ km/h with a front-wheel driven vehicle.

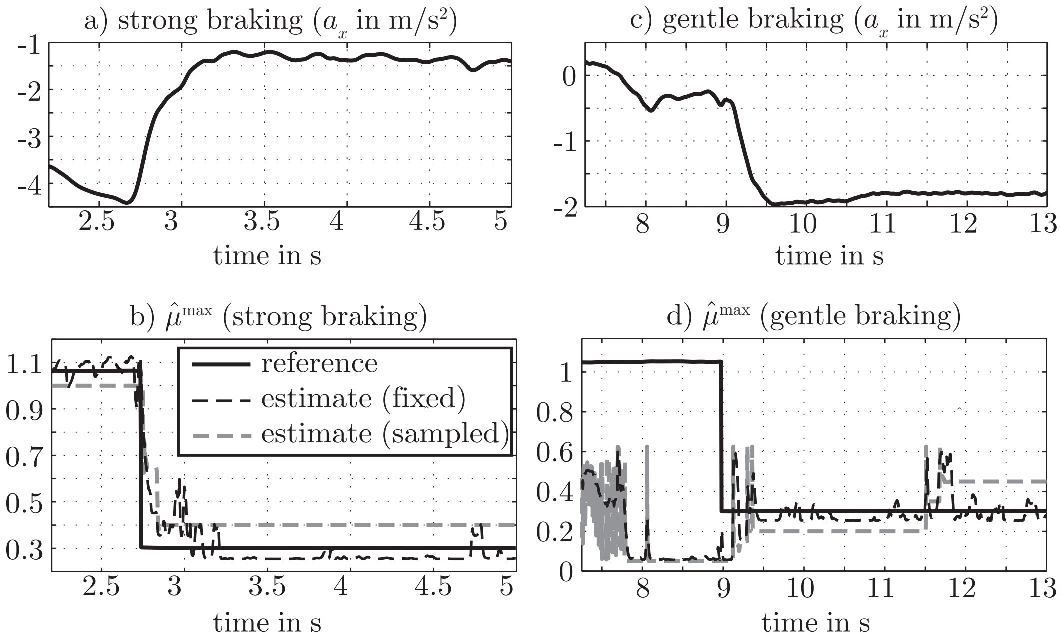

Figure 4. Acceleration profiles and estimates of $\mu^{\max}$ for rear left wheel on a μ *step* road surface are shown for strong braking starting at $v_x \approx 50$ km/h (left side) and gentle braking starting at $v_x \approx 40$ km/h (right side).

3.3 *Braking on μ split*

Figure 5 shows the estimates obtained during a braking manoeuvre on a μ *split* surface, with the left wheel being on the low-friction surface and the right wheel being on the high-friction surface. As with the comparison of hard and gentle braking, it can be seen that the high-friction surface cannot be detected at low body accelerations. On the low-friction surface, with increasing acceleration (about 7.5 s), the estimates improve. At about 8.5 seconds, the estimates increase compared to the reference value. This may be because the water film under the tire does not remain constant during strong braking at the physical limits. Thus, for short periods of time, higher accelerations can be achieved than would be expected. This effect is not considered at the reference value.

3.4 *Estimation errors*

Table 1 shows an overview on the mean absolute errors (MAE) and the maximum absolute errors (MAX) for the different manoeuvres and estimator strategies. Maximum deviations occur in the

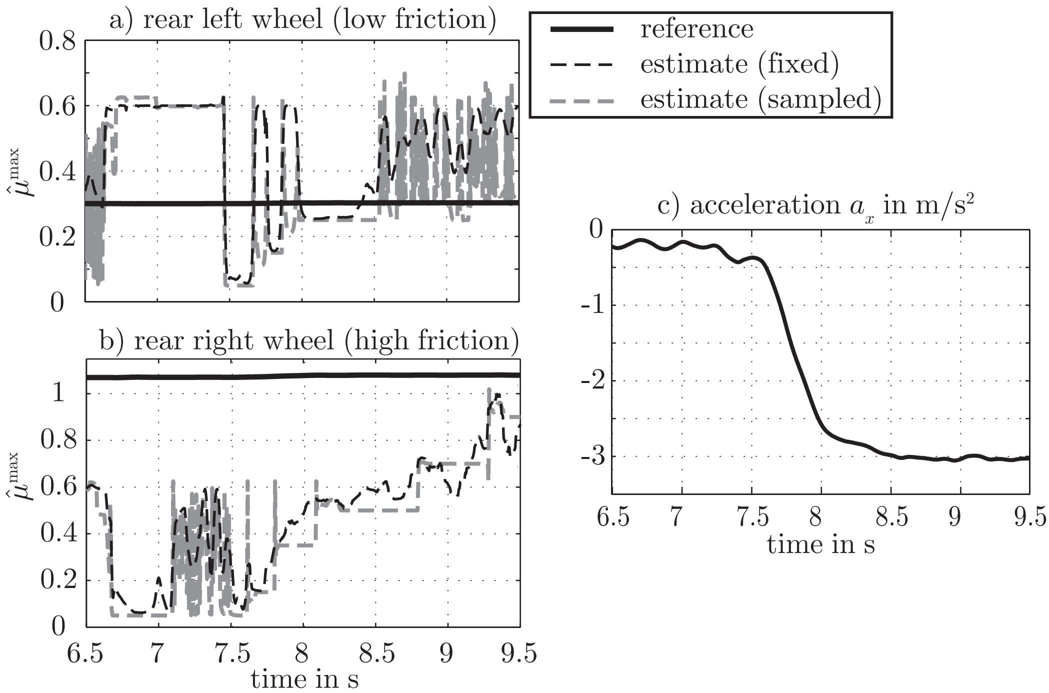

Figure 5. Estimates of $\mu^{\max}$ for μ *split* surfaces for rear left (low friction) and rear right wheel (high friction) shown on left side, which were obtained during the braking manoeuvre shown on right side starting at $v_x \approx 30$ km/h.

Table 1. Mean absolute errors (MAE) and maximum absolute errors (MAX) for different manoeuvres and estimation strategies (fixed and sampled particles)

manoeuvre	**road condition**	**particles**	**MAE**	**MAX**
acceleration	constant	fixed	0.17	0.79
acceleration	constant	sampled	0.08	0.15
braking, strong	μ *step*	fixed	0.06	0.75
braking, strong	μ *step*	sampled	0.1	0.7
braking, gentle	μ *step*	fixed	0.3	1.0
braking, gentle	μ *step*	sampled	0.36	1.01
braking	μ *split* (low friction)	fixed	0.2	0.35
braking	μ *split* (low friction)	sampled	0.16	0.4
braking	μ *split* (high friction)	fixed	0.6	1.01
braking	μ *split* (high friction)	sampled	0.65	1.02

small periods where the particles start with a uniform distribution, and thus show a low confidence, or at the first time step when μ changes (μ *step*). In general, the MAE are more meaningful to evaluate the estimates. It can be seen that in the cases with sufficient dynamic excitation in relation to the physical limits, the MAE are mainly within 0.1.

4 CONCLUSION

Reliable information on the current road and tire conditions is required in order to ensure safe driving at higher levels of automated driving. A method is presented to estimate road and tire conditions based on measurements of the vehicle's dynamic response. It is demonstrated that the proposed method provides high potential to improve current techniques for estimation of road and tire conditions based on vehicle dynamics measurements in certain driving conditions. Apart from measurements of the vehicle's longitudinal velocity, the sensor signals of a vehicle equipped with electronic stability control (ESC) were sufficient. To have sufficiently accurate values of the velocity, both GPS velocity and inertial measurements were used. Since the proposed method is based on the measurement of the dynamic reaction of the vehicle during driving, the estimation accuracy increases with the dynamic excitation. This means that for accelerations closer to the physical limits, the friction estimate is more accurate. Since current ADAS are developed to meet requirements on high-friction surfaces ($\mu^{\max}$ about 1), the detection of low friction surfaces is especially of interest. To detect these conditions, lower accelerations are sufficient than for the detection of high-friction surfaces. Another advantage of the proposed method is the inclusion of the tire condition rather than only the road condition, like e.g. with optical sensors. However, taking into account additional information like car-to-car systems or optical sensors (cameras, radar sensors) in future applications will enable achieving a robust estimate over a wide range of driving conditions.

REFERENCES

Boßdorf-Zimmer B. 2007. Nichtlineare Fahrzustandsbeobachtung für die Echtzeitanwendung. Dissertation thesis. Braunschweig University of Technology.

Eichberger A. 2011. Contributions to Primary, Secondary and Integrated Traffic Safety. Habilitation thesis. Graz University of Technology.

Gustafsson F. 1997. Slip-based tire-road friction estimation. *Automatica* 33(6): 1087-1099.

Hirschberg W. 2009. TMsimple: A simple to use tyre model. Technical report. Graz University of Technology.

Lex C. 2015. Estimation of the maximum coefficient of friction between tire and road based on vehicle state measurements. Dissertation thesis. Graz University of Technology.

Ray L. R. 1997. Nonlinear Tire Force Estimation and Road Friction Identification: Simulation and Experiments. *Automatica* 33: 1819-1833.

Simon D. 2006. The particle filter, chapter 15, p. 461-483. In: *Optimal State Estimation. Kalman, H_∞, and Nonlinear approaches*, John Wiley and Sons.